DIAMOND PHOTODETECTOR RESPONSE TO DEEP UV EXCIMER LASER EXCITATION

S.P. Lansley[1†]*, R.D. McKeag[2], M.D. Whitfield[3], N. Rizvi[3], and R.B. Jackman[1]

[1]Department of Electronic and Electrical Engineering, University College London, Torrington Place, London, WC1E 7JE, U.K.

[2]Centronic Limited, Centronic House, King Henry's Drive, New Addington, Croydon, CR9 0BG, U.K.

[3]Exitech Limited, Hanborough Park, Long Hanborough, Oxford, OX8 8LH, U.K.

Diamond photoconductive detectors have previously been shown to be suitable for detection of deep ultraviolet nanosecond-scale pulses from excimer lasers, which are to be used in next generation lithographic systems. Using simple test circuitry and low bias voltages easily measurable responses were observed when these detectors were illuminated with laser pulses at typical laser fluence levels. However, as the laser fluence is increased the detector response appears to broaden and change shape as well as increase in magnitude.

In this paper we present analysis of the response of these detectors. This analysis shows that over the laser fluence range used the magnitude of the detector response exhibited a linear response. By approximating the temporal evolution of the laser pulse and simulating the transfer characteristics of the test circuit it can be seen that the pulse broadening and shape change seen with increasing fluence can be explained by the test circuit. The shape of the detector response, therefore, closely resembles the temporal shape of the laser pulse, demonstrating that these devices are fast enough to give a true representation of 10- 15ns laser pulses at a wavelength of 193nm.

† now at Department of Engineering, University of Cambridge, Trumpington Street, Cambridge, CB2 1PZ, U.K.

1 INTRODUCTION

Diamond is a suitable material for the fabrication of photoconductive devices for operation in the deep ultraviolet region (< 225 nm) of the spectrum whilst remaining blind to visible wavelengths [1]. Improvements in the performance characteristics of devices fabricated from thin film polycrystalline diamond have made these structures suitable for a number of applications leading to commercial exploitation of this technology [2-4].

The high-speed response of photoconductive devices fabricated on both natural and synthetic diamond has been investigated at a variety of laser wavelengths; for example, natural diamond above [5-10] and below [10, 11] the bandgap of diamond, chemical vapour deposition (CVD) diamond above [10, 12-18] and below [10, 13, 19-22] the bandgap and high pressure high temperature (HPHT) diamond [10]. Of particular commercial interest is the response of diamond photoconductive device to pulses from excimer laser sources such as ArF (193 nm) and F_2 (157 nm); wavelengths chosen for future lithographic generations [23, 24]. At these wavelengths current silicon photodetectors exhibit poor UV sensitivity, negligible UV/visible discrimination and also poor radiation hardness [25]. CVD diamond UV photoconductors may offer a viable solution to these problems. However, potential devices need to show sufficient sensitivity and speed to be useful in high repetition rate excimer laser systems (1 kHz) and demonstrate stability to at least 10^8 pulses to satisfy industry requirements [25]. Previous work has shown that photoconductive structures on as-grown CVD diamond show relatively modest performance [26], but considerable improvement to the device characteristics can be obtained from a combination of careful device design and differing material treatments [2, 27]. The response of such devices to ArF [15-18] and F_2 [19] excimer laser pulses has previously been reported by the authors of this paper, and the response of natural diamond photodetectors to ArF laser pulses has been reported by other authors [7]. This paper analyses the response at 193 nm (ArF) of treated devices and examines the effect of the measurement circuit on the measured detector response.

2 EXPERIMENTAL

Free-standing polycrystalline diamond, grown using microwave plasma enhanced chemical vapour deposition, was used during the fabrication of these photoconductors. The films were about 100 μm thick, with typical grain size of 20-40 μm and random morphology. As previously reported [28], Raman spectroscopy carried out using a red He-Ne excitation source showed only the sharp characteristic peak of diamond at 1332 cm^{-1} with very little background and no evidence of any other structure. This diamond was cleaned using a standard acid treatment, which has been shown to remove any contamination and residual sp^2 from the surface, oxidize the surface and also remove the p-type conductive layer which can form on the surface of CVD diamond during the shut down phase of the growth reactor [29].

The photoconductors consisted of inter-digitated transducer structures with 15 electrode pairs on a 25 μm 1:1 mark to space ratio. These structures were patterned on the rough, growth surface of the diamond films using a photolithography process modified to cope with the large surface roughness of these films. Processing was carried out in a class 100 clean room and the gold contacts were deposited by thermal evaporation. After device patterning the samples were then subjected to a gaseous treatment which we have shown improves the leakage current and UV/visible discrimination of photoconductor devices based on the material and device structure used here. This treatment involves a two stage heat treatment in methane and then air and has been described in more detail elsewhere [2]. The results described in this paper come from devices that have been subjected to multiple consecutive treatments. Prior to laser pulse experiments these device were packaged in industry standard TO5 cans but without windows as standard windows absorb in the deep UV were these measurements are to take place.

The devices were placed directly in the beam of a 193 nm ArF excimer laser (Lambda Physik LPX200); these pulses typically had FWHM of 10-15 ns. A schematic diagram of the laser set-up has been given previously [16]. Laser fluence levels of between 0.1 and

1.5 $mJcm^{-2}$ were used, with the fluence being controlled by varying the angle of attenuator plates in the beam path. The response of the detectors to this laser irradiation was assessed using a 50 Ω impedance measurement circuit in series with a 50 Ω, 500 MHz storage scope (Tektronix TDS 3052) and a 9 V bias battery. For comparison of the pulse shape measurements were also taken using a vacuum photodiode as previously reported [16].

3 RESULTS & DISCUSSION

The responses of the devices given 3 and 7 treatments are shown in Figure 1 (a) and (b) respectively. The various curves correspond, in ascending magnitude, to laser fluences of 0.13, 0.23, 0.48, 1.03, and 1.45 $mJcm^{-2}$. The voltage plotted is the voltage obtained across the 50Ω of the digital oscilloscope, which is in series with the detector under test, thereby forming a potential divider circuit. All devices exhibited easily measurable response when illuminated by the laser pulses. The device given 3 treatments (Figure 1 (a)) shows increasing pulse height with increasing fluence, appearing to reach a maximum at about 8V. The shape of the response curve appears to change, flattening at the top and getting broader as the laser fluence is increased. Similar trends were seen for the device given 1 treatment and, to a slightly lesser extent, the device given 5 treatments. However, as shown for the device given 7 treatments, and similarly for the nine times treated device, a much more linear increase in peak height is seen with increasing fluence. The peak voltage as a function of the laser fluence is shown in Figure 2. Ideally we would expect the peak voltage to increase linearly with fluence but a non-linear relationship is seen, with saturation at about 8V for the more responsive devices, i.e. those given 1, 3, and 5 treatments.

The bias circuit used for these measurements simply consisted of a digital storage oscilloscope in series with the device under test and a 9V battery. This circuit acts a potential divider circuit with the output voltage being the voltage across the 50Ω of the oscilloscope; the output voltage, V_o, is $V_i*R_s/(R_s+R_d)$ where V_i is the bias voltage and R_s

and R_d are the resistances of the scope and device respectively. In the dark the resistance of the device under test is >GΩ and so the output voltage is very small. When the device is illuminated by the laser, its resistance drops dramatically, giving a measurable voltage drop across the oscilloscope. The conductance of the device under test should be proportional to the number of carriers available for conduction, and hence proportional to the laser fluence. Device conductance in the dark is much smaller than it is when illuminated by the laser and so we have approximated the device resistance by K_1/Φ, where Φ is the laser fluence and K_1 is a constant for each device, which should be related to the device responsivity at the laser wavelength. The potential divider equation thus becomes Equation 1.

$$V_o = \frac{V_i \Phi}{\frac{K_1}{R_s} + \Phi} \qquad \text{Equation 1}$$

Curve fits of the form of Equation 1 are shown in Figure 2. A linear region is seen at low fluence levels followed by a transition into a non-linear regime once the device resistance is comparable to the resistance of the oscilloscope. At the fluence level used during these measurements the devices given 1, 3, and 5 treatments are acting in the non-linear regime, whereas the devices given 7 and 9 treatments are still within the linear region. At the laser wavelength the responsivity of these devices varies over three orders of magnitude (the spectral responsivity of these devices has been reported previously [16]) as does K_1 and an inverse relationship between these two values is seen. This agrees with the assumption made that the device conductivity is linear with responsivity.

The laser pulse was measured by a vacuum photodiode; the full width at half maximum was about 11.5 ns. The pulse shape could be approximated by the sum of two Gaussian pulses, with the first pulse being 2-3 times taller than the second pulse. However, for simplicity, the laser pulse has been approximated as a single Gaussian pulse with magnitude equal to the laser fluence. The effect of the measurement circuit on a Gaussian pulse is simulated by replacing Φ in Equation 1 by a Gaussian pulse for each

fluence level used, using the curve fit parameters obtained from Figure 2. The simulated results for the devices given 3 and 7 treatments are shown in Figure 3 (a) and (b) respectively; the Gaussian pulse used was centred on zero and the results are plotted as a function of t/τ.

The results shown in Figure 3, along with similar simulations for devices given 1, 5, and 9 treatments, show very similar variations in peak height and pulse shape to the experimental result, for example those shown in Figure 1. The saturation of pulse height, broadening of the pulse and flattening of the pulse peak are all seen.

The full width at half maximum of a Gaussian pulse is $2\tau\sqrt{(\ln 2/\pi)}$, where τ is a measure of the width of the Gaussian pulse. However, Equation 1 has a highly non-linear effect as the magnitude of the pulse increases. This compresses the pulse more the higher up the pulse we look. Therefore the more compressed a pulse appears, the lower down the true pulse the full width at half maximum has been measured; effectively the full width at less than half maximum. Analysis of a Gaussian pulse modified according to Equation 1 yields a full width at half maximum equal to Equation 2, where Φ is the laser fluence, K_1 is as obtained from the curve fits shown in Figure 2 and R_s is the impedance of the oscilloscope. At zero fluence ($\Phi=0$) this equation gives the full width at half maximum of an un-modified Gaussian pulse.

$$FWHM = 2\tau\sqrt{\frac{\ln\left(2+\frac{\Phi}{K_1/R_s}\right)}{\pi}} \qquad \text{Equation 2}$$

The measured full width at half maximum is plotted at different fluence levels in Figure 4. The curve fits, which are plotted, are of the form of Equation 2, using the K_1 values obtained from the curve fits shown in Figure 2. The data shows an increase in FWHM with fluence for devices 1, 3, and 5 treated devices but no significant increase for the 7 and 9 times treated devices. A similar shaped variation of FWHM with fluence is shown

by the curve fits of Equation 2. The y-intercept values of the five curves have an average value of 11.6 ns, which correlates well with the average FWHM of the laser pulse as measured by the vacuum photodiode (11.5 ns).

4 CONCLUSIONS

The results reported here and previously have shown that easily detectable response to pulses from an ArF excimer laser can be obtained using a very simple measurement circuit. However, this measurement circuit has been shown to distort the response. Analysis shows the effect that this circuit has on the response and suggests that devices are capable of closely following the shape of the laser pulse on this time scale, with a linear response to the laser fluence. With such a simple circuit the detector can be used in a pulse-counting mode, or, by tailoring of the detector responsivity using gas treatments, a pulse-following mode over a range of fluence levels.

5 REFERENCES

[1] M.I. Landstrass, M.A. Plano, M.A. Moreno, S. McWilliams, L.S. Pan, D.R. Kania and S. Han, Diam. & Rel. Mater., **2**, 1033 (1993)

[2] R.D. McKeag, S.S.M. Chan and R.B. Jackman, Appl. Phys. Lett., **67,** 2117 (1995)

[3] M.D. Whitfield, R.D. McKeag, L.Y.S. Pang, S.S.M. Chan and R.B. Jackman, Diam.& Rel. Mater., **5,** 829 (1996)

[4] R.D. McKeag and R.B. Jackman, Diam. & Rel. Mater., **7**, 513 (1998)

[5] P.K. Bharadwaj, R.F. Code, H.M. van Driel and E. Walentynowicz, Appl. Phys. Lett., **43**, 207 (1983)

[6] J. Glinski, X.-J. Gu, R.F. Code and H.M. van Driel, Appl. Phys. Lett., **45**, 260 (1984)

[7] Y.S. Huo, X.J. Gu, R.F. Code and Y.G. Fuh, J. Appl. Phys., **59**, 2060 (1986)

[8] L.S. Pan, D.R. Kania, P. Pianetta and O.L. Landen, Appl. Phys. Lett., **57**, 623 (1990)

[9] P. Gluche, O. Kohn, M. Binder, M. Adamschik, W. Ebert, A. Vescan, E. Rohrer, C.E. Nebel and E. Kohn, Proceedings of the IEEE Cornell Conference on Advanced Concepts in High Speed Semiconductor Devices and Circuits, **VII-4**, 314 (1997)

[10] F. Foulon, P. Bergonzo, C. Borel, R.D. Marshall, C. Jany, L. Besombes, A. Brambilla, D. Riedel, L. Museur, M.C. Castex and A. Gicquel, J. Appl. Phys., **84**, 5331 (1998)

[11] P.-T. Ho, C.H. Lee, J.C. Stephenson and R.R. Cavanagh, Opt. Comm., **46**, 202 (1983)

[12] L.S. Pan, D.R. Kania, S. Han, J.W. Ager, M. Landstrass, O.L Landen and P. Pianetta, Science, **255**, 830 (1992)

[13] S. Salvatori, M.C. Rossi and F. Galluzzi, Carbon, **37**, 811 (1999)

[14] M.D. Whitfield, S.P. Lansley, O. Gaudin, R.D. McKeag, N. Rizvi and R.B. Jackman, Phys. Stat. Sol. (a), **181** (1), 121 (2000)

[15] M.D. Whitfield, S.P. Lansley, O. Gaudin, R.D. McKeag, N. Rizvi and R.B. Jackman, Diam. & Rel. Mater., **10**, 650 (2001)

[16] M.D. Whitfield, S.P. Lansley, O. Gaudin, R.D. McKeag, N. Rizvi and R.B. Jackman, Phys. Stat. Sol. (a), **185** (1), 99 (2001)

[17] M.D. Whitfield, S.P. Lansley, O. Gaudin, R.D. McKeag, N. Rizvi and R.B. Jackman, Proc. SPIE, **4274**, 40 (2001)

[18] M.D. Whitfield, S.P. Lansley, O. Gaudin, R.D. McKeag, N. Rizvi and R.B. Jackman, Diam. & Rel. Mater., **10**, 693 (2001)

[19] F. Foulon, P. Bergonzo, C. Jany, A. Gicquel and T. Pochet, Diam. & Rel. Mater., **5**, 732 (1996)

[20] F. Foulon, P. Bergonzo, C. Jany, A. Gicquel and T. Pochet, Nucl. Intrum. Methods A, **380**, 42 (1996)

[21] J.M. Marshall and A.S. Walters, Diam. & Rel. Mater., **8**, 2118 (1999)

[22] S. Salvatori, M.C. Rossi, F. Galluzzi, D. Riedel and M.C. Castex, Diam. & Rel. Mater., **8**, 871 (1999)

[23] www.sematech.org

[24] R. Harbison, Proceedings of the First International Symposium on 157 nm Lithography, May 8-11, Dana Point, California, U.S.A., **1**, 9-33 (2000)

[25] N. Rizvi, report by Exitech Ltd., part of Dti/EPSRC LINK project "INDDUV", London, U.K. (2000)

[26] P. Gonon, S. Prawer and D. Jamieson, Appl. Phys. Lett., **68,** 1238 (1996)

[27] O. Gaudin, S. Watson, S.P. Lansley, H.J. Looi, M.D. Whitfield and R.B. Jackman, Diam. & Rel. Mater., **8**, 886 (1999)

[28] H.J. Looi, R.B. Jackman and J.S. Foord, Appl. Phys. Lett., **72,** 353 (1998)

[29] B. Baral, S.S.M. Chan and R.B. Jackman, J. Vac. Sci. Tech., **A14,** 2303 (1996)

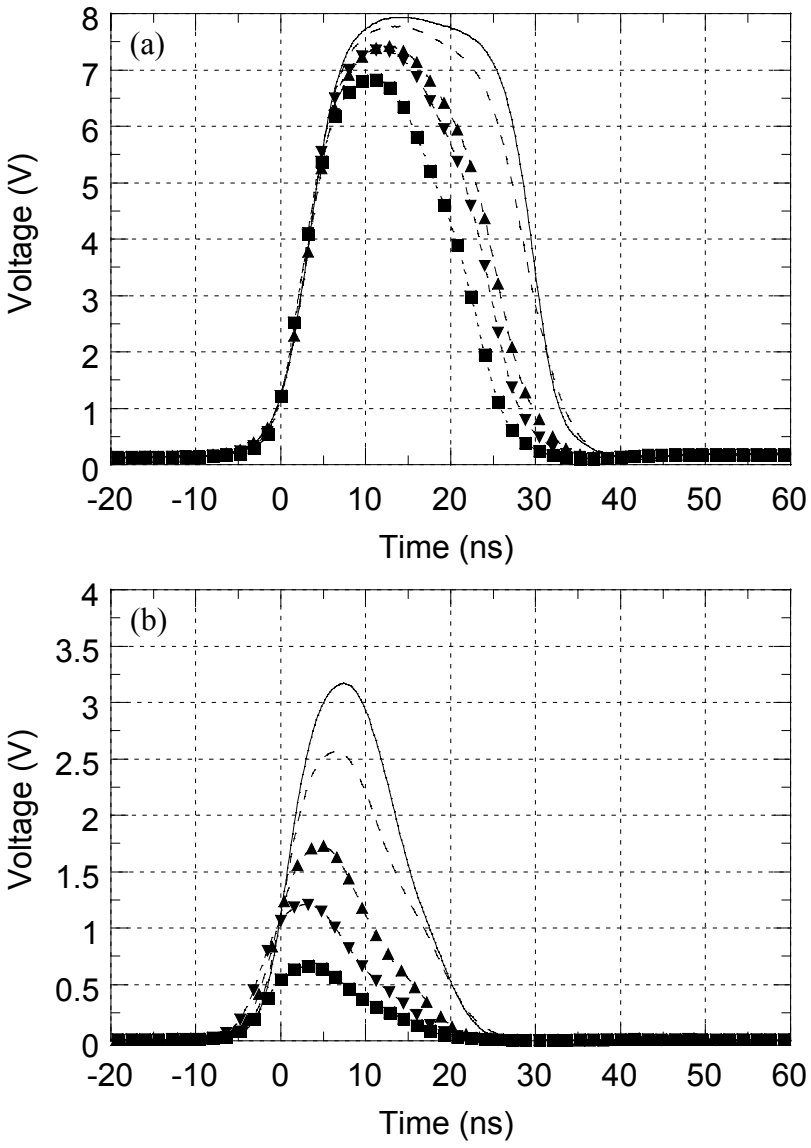

Figure 1 – Laser pulse response at 0.13 (■), 0.23 (▼), 0.48 (▲), 1.03 (dashed line) and 1.45 (solid line) $mJcm^{-2}$ for devices given (a) 3 treatments and (b) 7 treatments.

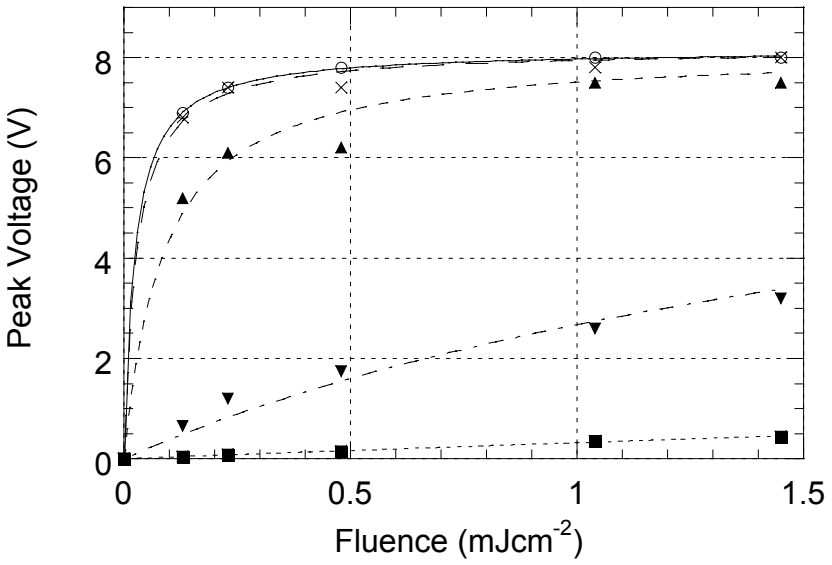

Figure 2 – Peak voltage versus laser fluence for devices given 1 (○), 3 (x), 5 (▲), 7 (▼) and 9(■) treatments. Curve fits of the form of Equation 1 are shown for each device.

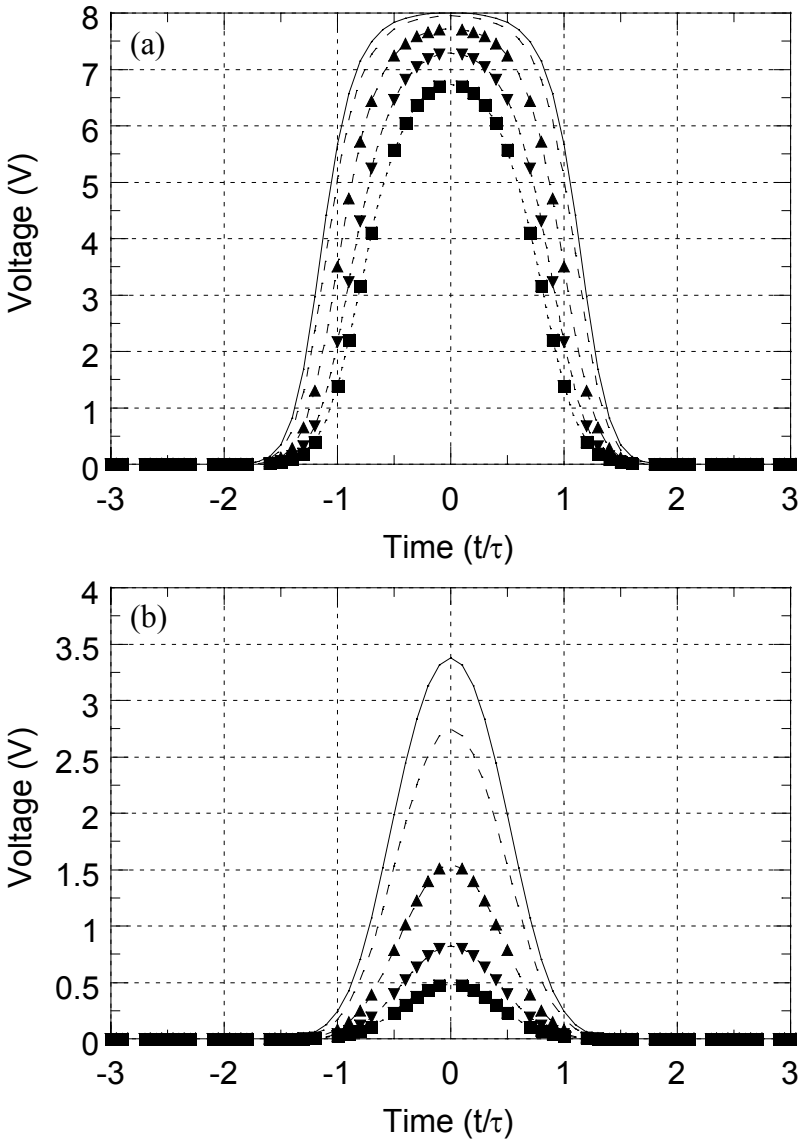

Figure 3 – Simulated response of the measurement circuit to a Gaussian pulse at 0.13 (■), 0.23 (▼), 0.48 (▲), 1.03 (dashed line) and 1.45 (solid line) $mJcm^{-2}$ for devices given (a) 3 treatments and (b) 7 treatments.

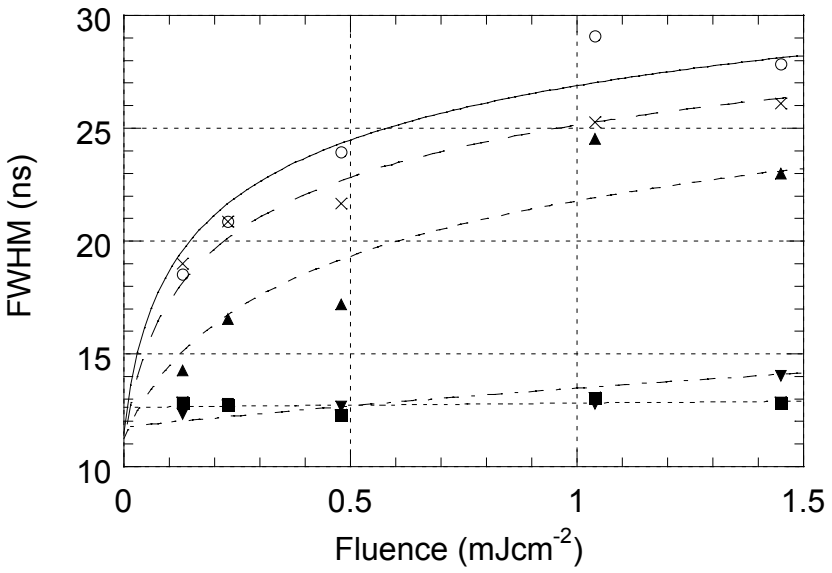

Figure 4 – Full width at half maximum versus laser fluence for devices given 1 (○), 3 (x), 5 (▲), 7 (▼) and 9(■) treatments. Curve fits of the form of Equation 2 are shown for each device.